ELSEVIER

Journal of Nuclear Materials 241–243 (1997) 696–700

journal of nuclear materials

Routes to divertor detachment in ASDEX Upgrade

C.S. Pitcher [a,b,*], A.W. Carlson [a], C. Fuchs [a], A. Herrmann [a], W. Suttrop [a], J. Schweinzer [a], M. Weinlich [a], ASDEX Upgrade Team [a], NBI Group [a]

[a] *Max-Planck-Institut für Plasmaphysik, IPP-EURATOM Association, D-85748 Garching, Germany*
[b] *CFFTP, Toronto, Canada*

Abstract

A simple analytic model of divertor radiation is used as a framework for identifying different routes to divertor detachment. Three means of achieving detachment are demonstrated experimentally including, increasing plasma density, purposely increasing the impurity level and increasing the scrape-off layer connection length. The resulting low electron temperatures in the divertor causes friction processes to dominate ionization in the recycling region, giving rise to plasma pressure loss along field lines. The pressure loss is in approximate agreement with simple analytic modelling.

Keywords: ASDEX Upgrade; Divertor plasma; 1D model; Analytic; Radiation energy sink

1. Introduction

The parallel power density in the scrape-off layer (SOL) upstream of the divertor of a future fusion reactor, such as ITER, is expected to be very large, $q_u > 1000$ MW/m^2 [1]. While geometrical factors, associated with the magnetic field and the divertor plate configuration, can reduce the power actually incident on the divertor plate surface q_{plate} by a factor of ≈ 100, the resulting power density is still too high for realistic heat removal schemes, where a practical limit is $q_{plate} < 5$ MW/m^2. Thus, means of reducing the parallel power density through volumetric losses must be found and the most likely candidate is radiative loss by impurities, either intrinsic or purposely added to the discharge.

In this paper we consider the routes by which impurity radiation in the SOL, particularly near the divertor, can be enhanced to alleviate the heat removal problem at the divertor plate. We start first with a simple analytic model, which provides a framework for the experimental results obtained in the ASDEX Upgrade (AUG) tokamak presented in later sections.

2. Simple model

We assume that the divertor and SOL are essentially opaque to recycling neutrals and that flow reversal is not present. In this case, power flows across field lines into the SOL and along field lines to the divertor by conduction. The parallel power flux density q is governed by the heat conduction equation,

$$q = -\kappa_0 T^{5/2} \frac{dT}{dx}, \tag{1}$$

where κ_0 is a constant, T is the plasma temperature in units of energy (we assume $T_e = T_i$) and x is the distance along the field line ($x = 0$ at the stagnation point or upstream location, which we take as the outside mid-plane, $x = L$ at the plate). If Eq. (1) is integrated from the upstream location 'u' to the target plate 't', we arrive at,

$$T_u^{7/2} - T_t^{7/2} \simeq \frac{7 q_u L}{2 \kappa_0}, \tag{2}$$

where we have assumed that the parallel power is approximately constant over most of the length of the flux tube. This is approximately valid, as detailed calculations have indicated, even in cases with high radiation on open surfaces, since such radiation tends to be localized near the divertor where densities are elevated.

* Corresponding author.

PII S0022-3115(96)00589-2

The volumetric loss of power by impurity radiation (we neglect hydrogenic radiation) is given by

$$\frac{dq}{dx} = -c_z n_e^2 L_z, \tag{3}$$

where c_z is the impurity concentration, n_e is the plasma density and L_z is the radiated power coefficient.

Combining Eqs. (1) and (3), and integrating from the stagnation point to the target plate we arrive at

$$q_u^2 - q_t^2 = \tfrac{1}{3}\kappa_0 c_z L_z p_u^2 \left(T_u^{3/2} - T_t^{3/2}\right), \tag{4}$$

where p_u is the upstream plasma pressure (ion + electron) and q_t is the parallel power density at the target plate. We assume that radiation loss by impurities occurs upstream of the recycling region, and specifically upstream of the frictional zone. We assume that the impurity concentration c_z and radiated power coefficient L_z are constant along the SOL. One can see immediately from Eq. (4) that the loss of power along the flux tube depends on the presence of a parallel temperature gradient and increases strongly with upstream pressure. Similar derivations have been given earlier in [2,3].

Using Eqs. (2) and (4), and making the approximation $T_u \gg T_t$, we derive the following simple expression

$$\left(\frac{q_t}{q_u}\right)^2 \approx 1 - \frac{14}{3}\frac{c_z L_z n_u^2 L}{q_u} \tag{5}$$

Detachment will occur when the power reaching the recycling region approaches zero, that is when

$$\tfrac{14}{3} c_z L_z n_u^2 L > q_u \tag{6}$$

The left-hand side of Eq. (6) is simply the spatially-integrated radiation based on the upstream density n_u. The enhancement factor $14/3 \approx 5$, accounts for the fact that most of the radiation occurs close to the divertor at densities substantially higher than n_u. Considering the assumptions and approximation made in the above, Eq. (6) is not meant to be accurate in a quantitative sense. Instead, it provides a 'qualitative' framework for detachment experiments.

3. Routes to detachment

Eq. (6) indicates five routes by which detachment through impurity radiation can be achieved:

1. raise the upstream plasma density n_u;
2. increase c_z by purposely adding impurities;
3. increase L_z by using impurities with higher radiation rates;
4. decrease the power flow in the SOL q_u;
5. increase the connection length L.

In the remainder of this paper we present experimental evidence for all five routes to divertor detachment in AUG. Ideally, it would be desirable to independently vary each of the above parameters, while maintaining the others fixed. This has been attempted in the experiments described below, with only partial success.

4. Effect of discharge density

Fig. 1a gives the divertor power balance in an Ohmic density scan in deuterium (consisting of separate steady-state discharges) with $I_p = 0.8$ MA, $B_t = 2.1$ T and ∇B drift away from the X-point. The dominant impurity in these discharges is carbon, probably produced from chemical sputtering at the walls, which results in a central carbon concentration c_z that is nearly independent of density ($Z_{eff} \approx 1.7$) [4].

The parallel power density q_u is determined by two methods. In the first, IR thermography measurements at the plate (under low radiation conditions) are used along with the known magnetic geometry. In the second, q_u is indirectly calculated using

$$q_u = \frac{q_{95} P_{SOL}}{4\pi a \kappa^{1/2} \lambda_P} \tag{7}$$

where q_{95} is the safety factor, P_{SOL} is the power flowing

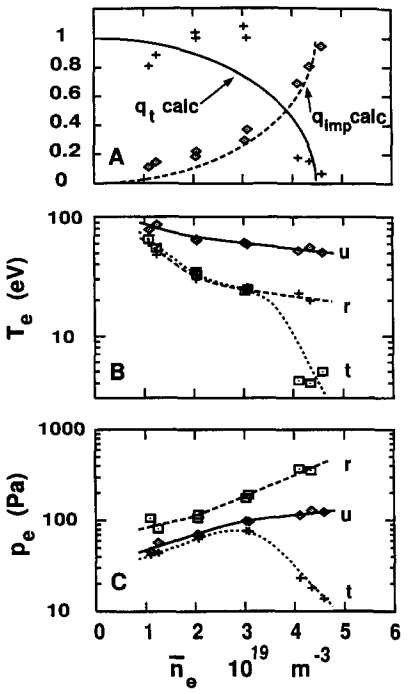

Fig. 1. SOL conditions from an Ohmic density scan: (A) Normalized parallel power density at the target plate (q_t, crosses) and impurity divertor radiation density (q_{imp}, diamonds). The lines are model results. (B) Electron temperatures at the upstream location (u) from ECE measurements, just above the recycling region (r) from a moving probe and at the target plate (t) from a built-in Langmuir probe. (C) Electron pressures corresponding to (B). The lines in (B) and (C) are only meant to guide the eye.

into the SOL, κ is the elongation and λ_P is the characteristic width for power flowing in the SOL.

In the density scan the upstream parallel power density is constant, $q_u \approx 13$ MW m^{-2}, based on the IR thermography (at low density), high resolution ECE T_e profiles at the mid-plane (at all densities) and P_{SOL} derived from bolometer measurements. We equate P_{SOL} with the power flowing to the divertor P_{DIV}, since the bolometers are not able to resolve SOL radiation from that in the confined plasma, i.e. $P_{SOL} \equiv P_{DIV} = P_{tot} - P_{rad,Xa}$, where P_{tot} is the total input power and $P_{rad,Xa}$ is the radiation above the X-point.

Shown in Fig. 1a is the peak parallel power density q_t as measured at the outer plate from IR thermography, normalized by 13 MW m^{-2}, and the radiated power in the divertor (below the X-point, $P_{rad,Xb}$ as measured by bolometers, normalized by P_{SOL}. Also included in Fig. 1a are the 'qualitative' predictions based on Eq. (5), using a connection length of $L = 25$ m, a constant impurity concentration $c_z = 0.02$ and a constant radiation coefficient $L_z = 2.5 \times 10^{-32}$ W m^3. While this value of L_z was chosen to give the best fit with the experimental results, it is close to what is expected based on non-coronal calculations [5]. The upstream density was taken to be $n_u = \bar{n}_e/3$, based on lithium beam measurements. The radiation density is calculated using $q_{imp} = q_u - q_t$.

The level of absolute agreement between the model and the experiment is fictitious, but the agreement in the trends, namely the non-linear increase of divertor radiation with discharge density and the corresponding rapid decrease in power to the plate, as predicted by Eq. (5), suggests the basic elements of the model are correct. The non-linear increase in radiation reflects the rapid increase in local plasma density that is a feature of a high-recycling divertor (conduction-limited and constant pressure along field lines in the radiating region).

Fig. 1b gives the separatrix electron temperature measured at various points in the SOL, including the upstream location 'u' from ECE, the outer target plate 't' from built-in Langmuir probes and a point approximately 10 cm above the outer plate, just above the recycling region, as measured by a moving Langmuir probe 'r'. Fig. 1c gives the corresponding electron pressures p_e, where in the case of the upstream location, the electron density for the pressure calculation is obtained from lithium beam measurements. One should note the absolute error in these measurements is ≈ 2, although the relative error is expected to be smaller.

In the case of the electron temperature, Fig. 1b, at low density and within experimental error, the SOL is isothermal. As the discharge density is increased, the temperatures start to diverge, with the upstream temperature T_u remaining approximately constant, as expected from Eq. (2), while T_t and T_r decrease together. At high density, T_t and T_r separate, with the target plate temperature reaching values as low as $T_t \approx 4$ eV.

The corresponding pressures indicate isobaric conditions, within the experimental error associated with probes (factor ≈ 2), throughout the density scan, except at the highest density, where a factor of ≈ 10 pressure drop between the upstream location and the plate is observed. The fact that the pressure at 'r', just above the recycling region, follows essentially the same trend as the upstream location 'u' suggests that the pressure loss region is located relatively close to the plate, i.e. vertically < 10 cm away.

5. Effect of extrinsic impurities

As discussed in Section 3, other routes to detachment include purposely adding impurities (Route 2), particularly with a higher radiation coefficient (Route 3), or decreasing the power flowing in the SOL (Route 4). Increasing the level of carbon (Route 1), using methane puffing, has been attempted without success on AUG, probably because carbon is a non-recycling impurity and is promptly removed from the plasma by depositing on surfaces. However, it has been possible to increase divertor radiation using recycling impurities with a higher radiation coefficient L_z, such as neon (Route 3). This, unfortunately, also results in an increase in neon-related radiation in the main plasma, thus reducing q_u and mixing Routes 3 and 4.

Fig. 2 gives an example of neon puffing for an L-mode

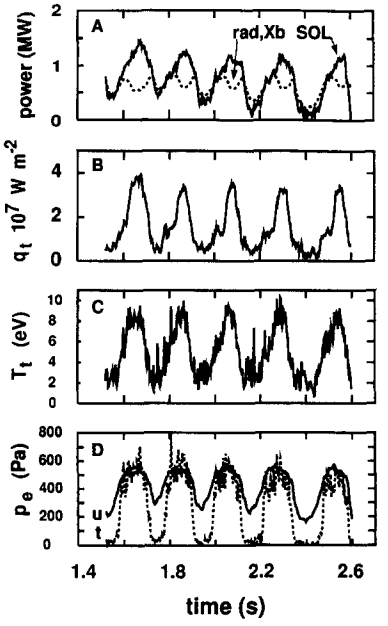

Fig. 2. SOL conditions in an L-mode discharge with neon: (A) Power entering the SOL P_{SOL} and radiation below the X-point P_{rrad,X_b}. (B) Peak parallel power density at the outer plate q_t. (C) Corresponding electron temperature at the plate T_t. (D) Electron pressure at the upstream (u) and target plate (t) locations.

discharge, where the input power and plasma density were kept constant at 3.5 MW and 5.5×10^{19} m^{-3}, respectively, while a neon valve was oscillated at a frequency ≈ 5 Hz. The resultant neon radiation in the main plasma caused a modulation of P_{SOL}, as derived using bolometers, by a factor 4, Fig. 2a. Also shown for comparison is the divertor radiation (below the X-point, $P_{rad,Xb}$). Within experimental error, essentially all of the power entering the divertor is radiated when the neon level is maximal, while the power reaching the divertor plates when the neon level is minimal is 0.6 MW. The radiation level is clearly anti-correlated with the (parallel) power density q_t and electron temperature T_t at the separatrix at the outer plate, as determined from IR thermography and a built-in Langmuir probe, Fig. 2b and c, respectively.

Also included in Fig. 2d is the separatrix electron pressure p_e at the upstream location, as determined by ECE and lithium beam, and at the plate from Langmuir probes. The modulation in P_{SOL} causes a modulation in the upstream electron temperature T_u, with little effect on the upstream density n_u, resulting in a factor of 2 modulation in the pressure. The corresponding modulation in the pressure at the plate is a factor ≈ 20.

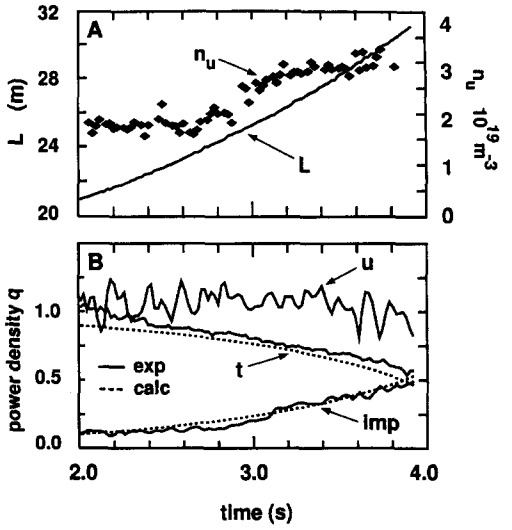

Fig. 3. SOL conditions in an H-mode current ramp-down discharge: (A) Connection length from outer mid-plane to outer target plate, upstream separatrix density from lithium beam measurements. (B) Normalized parallel power densities at the upstream (u) and target plate (t) locations, impurity divertor radiation density (imp) and model results.

6. Effect of connection length

The last route to detachment is to increase the connection length L, Eq. (6). This has been demonstrated in a current ramp-down experiment in an H-mode discharge with $B_t = 2.5$ T, ∇B drift towards the X-point, $P_{tot} = 5$ MW and $\bar{n}_e = 8.0 \times 10^{19}$ m^{-3}, all maintained constant while the plasma current was reduced from 1.2 MA to 0.8 MA over a period of 2 s. Fig. 3a gives the variation of the connection length L (outside mid-plane to outer plate) and separatrix plasma density n_u from lithium beam measurements. While the connection length increases from $L = 21$ m to $L = 32$ m during the ramp-down, unfortunately, the separatrix density also changes, increasing by 60%, despite $\bar{n}_e$ being maintained constant by the feedback system. As a consequence, the changes in the power balance in the divertor are a result of both the change in connection length as well as in n_u.

The change in connection length, i.e. q_{95}, also influences the parallel power density according to Eq. (7), but when changes in P_{SOL} and λ_P are taken into account the resulting q_u is virtually constant as the connection length is increased, Fig. 3b. Also given in the figure is the peak parallel power density q_t as measured at the outer plate from IR thermography, normalized by $q_u = 80$ MW m^{-2}, and the radiated power in the divertor (below the X-point, $P_{rad,Xb}$) as measured by bolometers, normalized by P_{SOL}. In this case, the reduction in parallel power at the plate is modest, a factor ≈ 2, although the increase in divertor radiation is substantial, a factor ≈ 5.

Also included in the figure are the predictions for the power to the plate and the radiation based on Eq. (5), the experimental measurements of L and n_u (somewhat smoothed), a constant impurity concentration $c_z = 0.02$ and a constant radiation coefficient $L_z = 2.5 \times 10^{-32}$ W m^3. The c_z and L_z values are the same as used in Section 4 for Ohmic discharges, and similarly, the experimental Z_{eff} is comparable in these H-mode discharges. Surprisingly good absolute agreement is obtained between the simple model and the experimental measurements, and is probably fortuitous given the approximations and uncertainties. Of more importance is the agreement in the trends and the point that both the increase in connection length and the upstream density contribute, roughly in equal measure, to the increase in divertor radiation and the corresponding decrease in power to the plate q_t.

7. Pressure loss factor f_m

Until this point 'detachment' has been defined in terms of power losses based on impurity radiation. It can be shown that high radiation levels, i.e. with $q_t/q_u < 0.2$, cannot be attained unless, in addition to radiative loss, there is plasma pressure loss [6,7], such as that illustrated in Fig. 1c and Fig. 2d. Conversely, significant pressure loss is unlikely to occur unless strong radiative cooling upstream of the frictional zone also occurs [8]. This pressure loss appears to be consistent with ion–neutral friction in the recycling region close to the plate, due to elastic and charge-exchange collisions, which start to dominate ionization at low values of electron temperature [8].

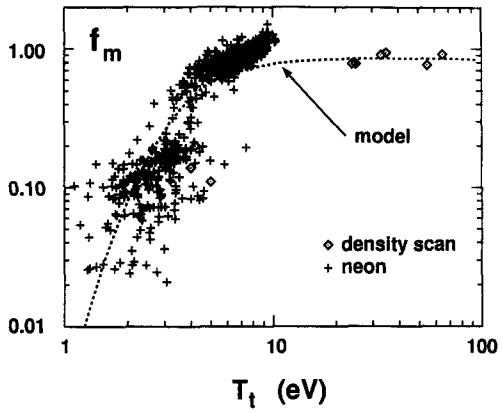

Fig. 4. Pressure loss factors f_m versus target plate electron temperature T_t from the Ohmic density scan, the L-mode discharge with neon and model prediction.

A simple and convenient analytic expression for the plasma pressure loss f_m across an isothermal recycling region is [7,9,10]

$$f_m \equiv \frac{2n_t T_t}{n_u T_u} = 2\left(\frac{\alpha}{\alpha+1}\right)^{(\alpha+1)/2}, \tag{8}$$

where

$$\alpha \equiv \frac{\langle \sigma v \rangle_i}{\langle \sigma v \rangle_i + \langle \sigma v \rangle_m} \tag{9}$$

where $\langle \sigma v \rangle$ are the rate coefficients for ionization (i) and momentum loss (m, including both elastic and charge-exchange collisions), given by [11]. To a first approximation, α, and therefore the pressure loss f_m, as shown in Fig. 4, depend only on the electron temperature in the recycling region, assumed to be the plate temperature T_t. In reality, the ionization will tend to occur in regions of higher T_e, somewhat upstream of the cooler region where the momentum transfer tends to occur.

Also included in Fig. 4 are experimental pressure loss factors taken from Figs. 1 and 2. As expected, at high values of electron temperature, i.e. $T_t > 10$ eV, where ionization dominates friction processes, little pressure loss is found, with $f_m \approx 1$, within experimental error. The rapid decrease of f_m at low values of T_t, in agreement with Eq. (8), is strong evidence supporting the hypothesis that the pressure loss is related to changes in atomic physics processes. Although the results appear to be explained by elastic and charge-exchange collisions, we cannot rule out, based on this data, a role played by electron–ion volume recombination [12,13].

8. Conclusions

There appear to be a number of routes by which divertor detachment induced by impurity radiation can be achieved. These include, (1) increasing the discharge density at constant impurity concentration, (2) purposely increasing the impurity level and (3) increasing the connection length. These methods enhance the level of impurity radiation in the divertor, as expected from simple analytic modelling, thus decreasing the power reaching the divertor plate.

High radiation levels, resulting in low divertor plate powers, necessarily imply low electron temperatures T_t in the recycling region close to the plate. With $T_t < 5$ eV, significant plasma pressure loss is expected across the recycling region, is found in experiment and is in approximate agreement with simple modelling based on friction resulting from ion–neutral elastic and charge-exchange collisions.

Acknowledgements

The authors are thankful for advice from Professor P.C. Stangeby, Dr. J. Neuhauser, Dr. R. Schneider, Dr. K. Borrass and Dr. D. Coster. C.S.P. is thankful for personal support from the Canadian Fusion Fuels Technology Project (CFFTP).

References

[1] G. Janeschitz, K. Borrass, G. Federici et al., J. Nucl. Mater. 220–222 (1995) 73.
[2] L.L. Lengyel, IPP Garching Report 1/191 (1981).
[3] M. Shimada et al., JAERI Report, JAERI-M 9862 (1981).
[4] A. Kallenbach et al., Nucl. Fusion 34 (1994) 1557.
[5] D. Post, J. Nucl. Mater. 220–222 (1995) 143.
[6] K. Borrass and G. Janeschitz, Nucl. Fusion 34 (1994) 1203.
[7] C.S. Pitcher and P.C. Stangeby, Plasma Phys. Control. Fusion (1997), submitted.
[8] P.C. Stangeby, Nucl. Fusion 33 (1993) 1695.
[9] S.A. Self and H.N. Ewald, Phys. Fluids 9 (1966) 2486.
[10] C.S. Pitcher et al., EPS Conf. on Plasma Physics and Controlled Fusion (Bournemouth, 1995) pp. 111–245.
[11] R.K. Janev et al., Elementary Processess in Hydrogen–Helium Plasmas (Springer-Verlag, Berlin, 1987).
[12] K. Borrass, D. Coster, D. Reiter and R. Schneider, these Proceedings, p. 250.
[13] S.I. Krasheninnikov, A.Yu. Pigarov and D.J. Sigmar, in: The Proc. Plasma Edge Theory Conf. (1995).